Static strengths of Ta and U under ultrahigh pressures

S. T. Weir, J. Akella, C. Ruddle, T. Goodwin, and L. Hsiung
Lawrence Livermore National Laboratory, University of California, P. O. Box 808, Livermore, California 94551
(Received 22 April 1998)

We have performed high-pressure strength experiments on tantalum and uranium using a diamond-anvil cell. These experiments determined the flow stresses of tantalum and uranium at room temperature and in the low strain rate limit ($\varepsilon' < 10^{-6}$ sec^{-1}) by using x-ray diffraction to measure the pressure gradients in the samples. We find that the flow stresses increase dramatically with increasing pressure and strain, with the flow stress of Ta reaching 10.3 GPa at a pressure of 85.8 GPa and an estimated strain of ≈90%, and the flow stress of U reaching 19.8 GPa at a pressure of 109.0 GPa and an estimated strain of ≈70%. With further increases in pressure and strain, the flow stresses decrease. This apparent strain-softening effect has also been observed in static high-pressure flow stress experiments on other materials, and has been suggested to be due to either material damage or preferred orientation of grains induced by large strains. [S0163-1829(98)05141-8]

I. INTRODUCTION

The study of material strength under ultrahigh pressures is an important subject of both technological and scientific interest. The technological interest stems from the need to understand the flow properties of shocked materials, and the desire to design static high-pressure devices capable of achieving higher pressures. Studies of high-pressure material strength are also important to geology, since the convective deformation of the mantle depends on the rheology of the materials in the Earth's interior. Finally, from a fundamental materials science and physics perspective, the relationship between material strength, elastic constants, and microstructure is of great interest, and can lead to new insights into the mechanisms of plastic flow under various pressure-temperature conditions.

A great deal of research into the effects of pressure on the strength and ductility of metals has been performed at pressures up to around 3 GPa using pressure vessels.[1–3] For metals, it was found that the application of high pressures tends to increase both strength and ductility. The increase in the yield strength is due to the fact that the shear modulus G increases with increasing pressure, causing higher stress fields about the dislocations. Thus, higher pressures inhibit dislocation movement and plastic flow, resulting in higher yield strengths and flow stresses. This pressure-hardening effect can be very significant at Mbar pressures.

It is also known that the application of high pressures can enhance the ductility of metals and, in fact, sudden pressure-induced brittle-to-ductile transitions have been reported in several metals.[4] Studies by Bridgeman[1] showed that the application of pressures in the range of 0.7–3.0 GPa resulted in remarkable increases in the ductilities of nickel, molybdenum, and tungsten. Tungsten, for example, is a brittle metal at atmospheric pressure, but could be plastically strained by over 100% under a pressure of 2.8 GPa.

It is desirable to extend strength studies on metals to much higher pressures than the pressure vessel limit of ≈3 GPa for several reasons. First, the shear modulii of most metals at 3 GPa are nearly identical to their zero-pressure values, and so the pressure-hardening effect is very difficult to observe at these pressures. An estimate based on recent first-principles calculations of Ta (Ref. 5) reveals that the shear modulus G increases by only about 3% from $P = 0-3$ GPa. Thus, while pressure vessel experiments are valuable for studying certain features of plastic deformation under high hydrostatic pressure, such as ductility enhancement and strain-hardening enhancement, for pressure-hardening studies of metals it is desirable to apply pressures of at least 10–50 GPa. Static strength studies in this high-pressure range are also applicable to the modeling and analysis of dynamic experiments involving high explosives since metals in these experiments are usually subjected to pressures of 25 GPa and higher. While the strain rates of our static experiments are much lower than those in dynamic experiments ($\varepsilon' \ll 1$ sec^{-1} vs $\varepsilon' > 10^5$ sec^{-1}), in both types of experiments dislocation generation and movement is the dominant deformation mechanism, and so static experiments can yield valuable fundamental insights.

The generation of static high-pressure yield strength data at pressures of 25 GPa and higher is especially timely since with recent advances in high speed computing, computational efforts are emerging involving the multiscale modeling of material strength in metals.[6,7] This multiscale work is an ambitious combined approach involving the modeling of dislocations, grain boundaries, and other defects at the atomistic scale, microscale, and mesoscale. Such efforts will greatly benefit from the benchmarks provided by ultrahigh-pressure yield strength data. For example, it has been suggested that at least some high-pressure brittle-to-ductile transitions are due to the pressure-induced activation of new slip systems.[4] If so, the ability to theoretically or computationally predict these transitions would be an important step forward in modeling material deformation at high pressures.

The study of static high-pressure yield strengths to 100 GPa and higher using diamond-anvil cells (DAC's) is a nascent field of study, and so the strengths of only a few metals have been studied thus far in DAC's to ultrahigh pressures. In this paper we report on the study of the metals tantalum (Ta) and uranium (U) to pressures up to 200 GPa.

II. EXPERIMENT

Our strength studies were performed on samples which were pressurized and plastically deformed in a diamond-

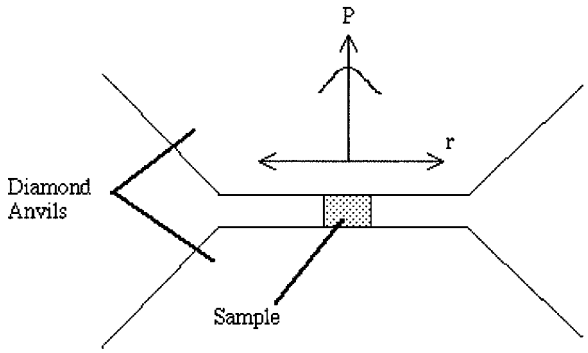

FIG. 1. Schematic of the sample region of a DAC. The sample is initially approximately 50 μm in diameter and 18–50 μm thick. 7° bevels are not shown.

anvil cell. Figure 1 shows a schematic of the sample region of the DAC. The anvils had 300 μm culets, central flats ranging from 50–100 μm, and bevel angles of 7°. For the Ta experiments, the sample was a thin foil (initial thickness=25 μm, Alpha Products Inc., 99.95%) which was acid etched to remove the oxide layer. For U, the sample was also a thin foil (initial thickness=25 μm, Goodfellow Inc., 99.9%). The initial grain size was <5 μm.

To determine the flow stress of the sample while under high pressure, we used *in situ* microprobe x-ray diffraction to measure the maximum radial pressure gradient $\partial P/\partial r$ in the Ta or U sample. X-ray diffraction directly gives the unit cell compression V/V_0, which in turn can be related to the local pressure by means of the isothermal P-V equations-of-state of Ta (Ref. 8) and U.[9] The diameter of the collimated x-ray beam was approximately 10 μm. Figure 2 shows some pressure gradient data taken on U. For a sample being compressed in the geometry shown in Fig. 1, it can be shown that σ_{rz}, the maximum shear stress in the sample, can be related to the radial pressure gradient by[10,11]

$$\sigma_{rz} \approx \frac{h}{2}\frac{\partial P}{\partial r}, \tag{1}$$

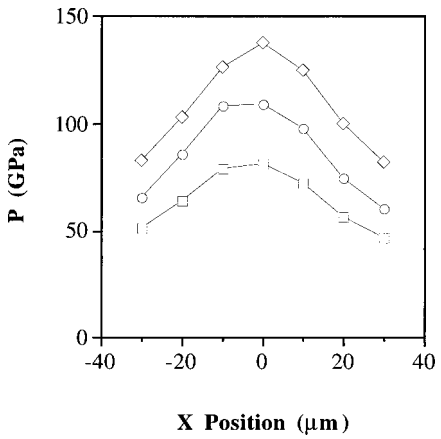

FIG. 2. Pressure vs collimator x position (U sample). Data shown here was taken at three different pressure loadings represented by the three different symbols.

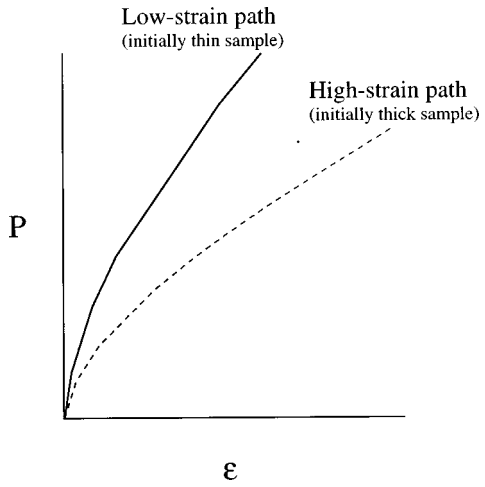

FIG. 3. Relative pressure-strain paths for DAC samples having different initial thicknesses.

where h is the sample thickness. This equation was derived by applying stress balance equations to the sample geometry shown in Fig. 1, and assuming that the geometry is axially symmetric and that the sample is being compressed between flat, rigid anvils with a no-slip boundary condition between the sample and the anvils. This no-slip boundary condition means that the diamond anvils serve to anchor the gasket and inhibit outward gasket flow, which is important for achieving Mbar pressures.

Two important approximations were made in order to integrate the stress balance equation and obtain Eq. (1). These are (i) that the normal stresses do not vary appreciably as a function of the axial z position and (ii) that the radial normal stress (σ_{rr}) is approximately equal to the azimuthal normal stress ($\sigma_{\theta\theta}$). Based on experimental observations, these ap-

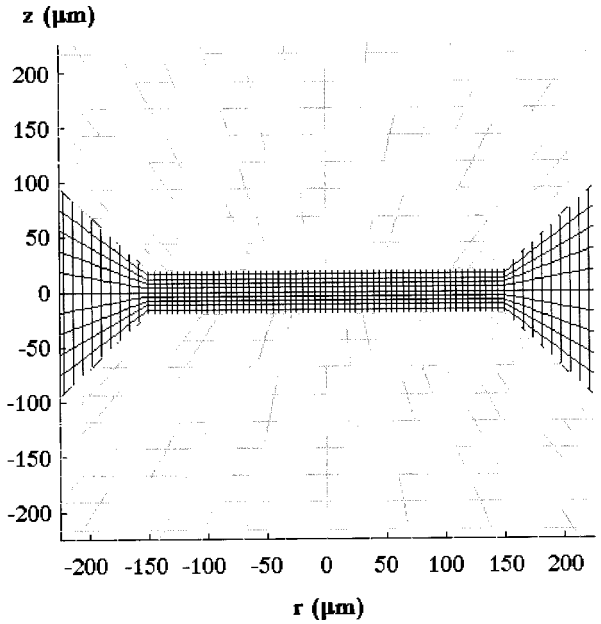

FIG. 4. Initial mesh pattern for the NIKE2D diamond-anvil cell simulation. This is a two-dimensional simulation with the axis of rotational symmetry along $r=0$. The metal gasket is sandwiched above and below by two diamond anvils.

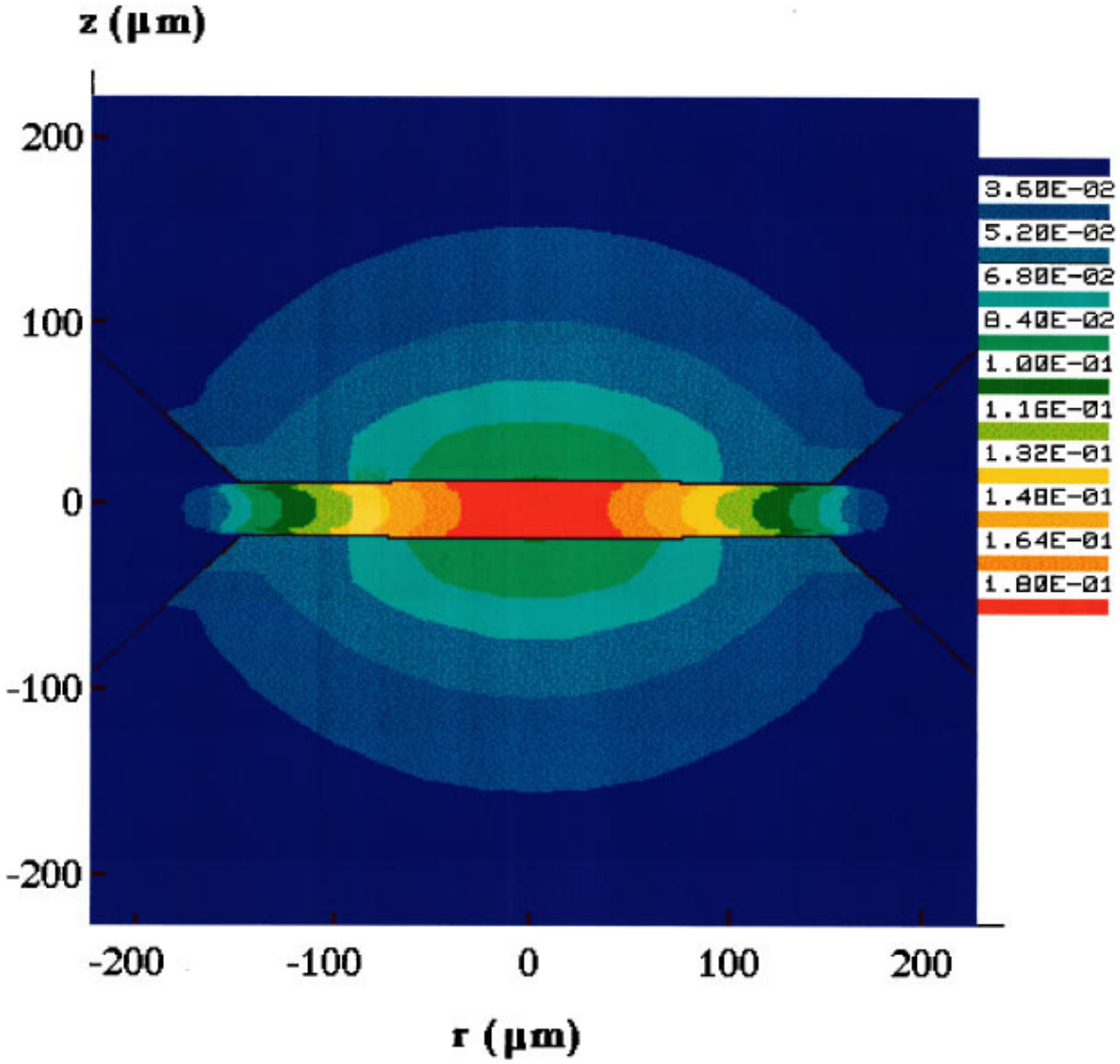

FIG. 5. (Color) Pressure plot for the NIKE2D diamond-anvil cell simulation. Gasket thickness has been compressed from 40 to 31 μm. The legend on the right side of the plot gives the pressures in Mbars.

proximations appear valid.[11] Our finite element simulations presented in the next section also support the validity of these approximations.

By applying the Tresca yield criterion, the flow stress σ_0 of the sample is given by $\sigma_0 = 2\sigma_{rz}$ or

$$\sigma_0 \approx h \frac{\partial P}{\partial r}. \tag{2}$$

The value of h was measured during the initial loading and after the DAC had been downloaded from its maximum pressure point. To obtain the thickness of the sample at the maximum pressure point, we downloaded the sample, measured the gasket thickness with a microscope, and then took into account the elastic expansion of the sample during decompression by correcting the zero-pressure measured thickness with the equation of state of the sample. Obtaining the *in situ* thicknesses h at intermediate pressure points would have required downloading the DAC, measuring the sample's thickness, and then reloading a new sample for each pressure point, a very time consuming task and one which would have resulted in very inefficient utilization of the limited available synchrotron x-ray beam time. Therefore, we instead estimated the gasket thicknesses at intermediate pressures by linearly interpolating the sample thickness between its thickness at ambient pressure and its thickness at maximum pressure. According to experimental observations and our finite element calculations (see next section), this is a reasonable approximation. Still, this approximation is a significant source of error in our experiments, and we estimate the uncertainty in the thicknesses to be $\approx$30%.

It should be noted that in the DAC sample geometry of Fig. 1, the sample is being pressurized and plastically strained simultaneously, and so both pressure hardening and strain hardening are operative in determining the strength of the sample. If the sample thickness decreases by about a factor of 2, which is typical in going from zero pressure to 100 GPa, we estimate that the sample undergoes roughly 100% strain.[12] This pressure-strain path can be varied somewhat by varying the initial starting sample thickness. Since we find that the final thickness at 100 GPa is approximately 10 μm, regardless of the starting thickness, larger starting

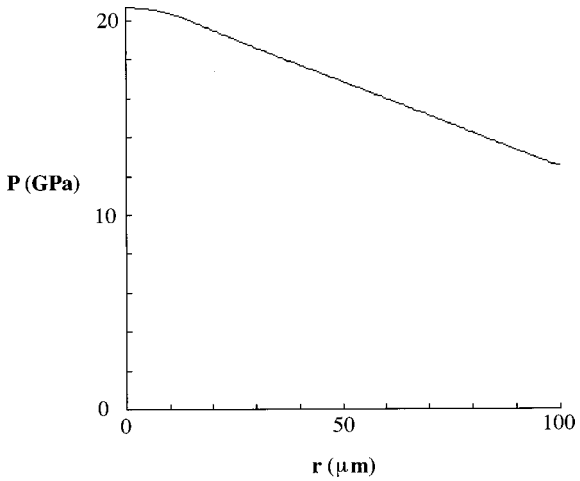

FIG. 6. Pressure vs radial position plot. The pressure is plotted at $z=13$ μm, which is near the gasket-diamond interface.

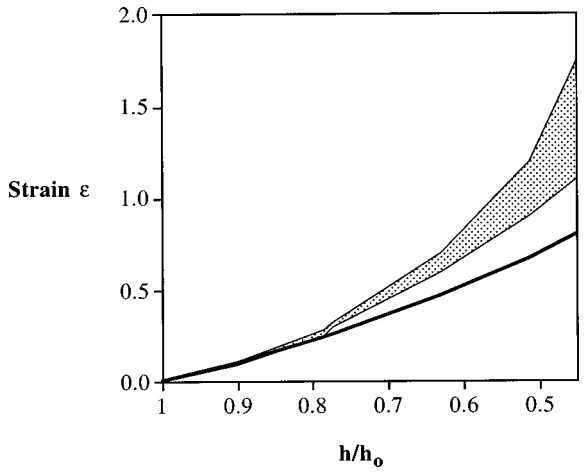

FIG. 7. Equivalent plastic strain vs normalized gasket thickness h/h_0. The estimated sample strain on the basis of NIKE2D simulations is represented by the shaded region. The solid line gives the estimated strain based on the equation $\varepsilon=\ln(A_0/A)$ for uniform one-dimensional strain.

thicknesses result in greater amounts of plastic deformation and strain as the sample is pressurized. Figure 3 shows the relative pressure-strain paths for two samples having different initial thicknesses.

To explore the effect of different pressure-strain paths on the strength of the sample, we performed two runs on Ta using different starting thicknesses of 25 and 50 μm, which provide ''low-strain'' and ''high-strain'' data, respectively. For U the initial thickness was 19 μm.

III. NIKE2D FINITE ELEMENT SIMULATIONS

We performed a number of NIKE2D (Ref. 13) finite element simulations of our experiments in order to gain a better understanding of the stresses and strains present in the sample, and of how our strength measurements may be affected by these stress and strain distributions. In particular, we were interested in investigating the validity of the pressure gradient method of determining sample strength in a DAC, and in estimating the amount of equivalent plastic strain in the sample as it undergoes pressurization.

Accurately simulating the compression of a metal gasket to Mbar pressures in a DAC is a difficult task because there is very limited information about the strengths of metals under such extreme stress and strain conditions. Previous NIKE2D simulations[14,15] have attempted to accurately model DAC behavior and to calculate, for example, the sample pressure as a function of applied force for the purpose of making direct comparisons to experiment. Our purpose here is much more limited in scope, and we confine ourselves to the study of those features which are relatively insensitive to the constitutive model used for the gasket, such as the equivalent plastic strain of the gasket as a function of its thickness. Therefore, we used a simple incompressible elastic-plastic model with no strain hardening or pressure hardening. The Young's modulus was set to $E=100$ GPa and the yield strength was set to $\sigma_y=2.00$ GPa. For the diamond anvil, we used a linear, isotropic, elastic model with shear modulus $G=1005$ GPa and Poisson's ratio $\nu=0.104$. The initial mesh pattern is shown in Fig. 4. The initial thickness of the gasket between the anvils was 40 μm, and the anvil culets were 300 μm in diameter. No-slip boundary conditions were imposed on the gasket-diamond interface.

The gasket is pressurized by forcing the anvils together. In our simulation we compressed the gasket thickness by abut 25% (thickness=31 μm), and examined the induced stress distributions and the strain. Figure 5 shows the pressure distribution at this compression. For reasons already state, we made no attempt to accurately model the magnitudes of these pressures. Rather, our interest here was on the spatial variations and gradients of the pressure, and on the relative values of the normal stresses. We now examine the two assumptions made in the flow stress study of MgO by Meade and Jeanloz.[11]

Assumption (1). There are no significant variations of the normal stresses in the gasket in the axial direction. We find, in fact, that the normal stresses change very little in the axial direction. At a radius $r=50$ μm, the normal stress σ_{zz} varies by $<3\%$ in the axial direction. For σ_{rr} and $\sigma_{\theta\theta}$, the variation is $<10\%$.

Assumption (2). The difference $\sigma_{rr}-\sigma_{\theta\theta}$ is small. At $r=50$ μm, $|\sigma_{rr}-\sigma_{\theta\theta}|/|\sigma_{rr}|<0.01$ which is small enough to be negligible in the stress balance equation. Values of the normal stresses at $r=50$ μm were used here, but the results are essentially the same for other radii near the center of the culet.

As a final test, we examined the validity of Eqs. (1) and (2), the flow stress equations used in analyzing our experimental data. Figure 6 shows the pressure vs radial distance near the gasket-diamond interface when the gasket thickness was compressed to $h=31$ μm. For radii greater than about half the gasket thickness, the radial pressure gradient is almost constant. At $r=30$ μm, the radial pressure gradient is $dP/dr=0.067$ GPa/μm. Therefore, $(h/2)(dP/dr)=1.04$ GPa. The simulation gives a shear stress of σ_{rz} of 1.02 GPa at the same location ($r=30$ μm; $z=13$ μm), so Eq. (1) holds quite well. In examining Eq. (2), we find that the simulation gives 2.08 GPa for the quantity on the right-hand side of the equation. This agrees very well with the yield strength of $\sigma_Y=2.00$ GPa used in the elastic-plastic model of the gasket.

We also used NIKE2D to estimate the amount of plastic

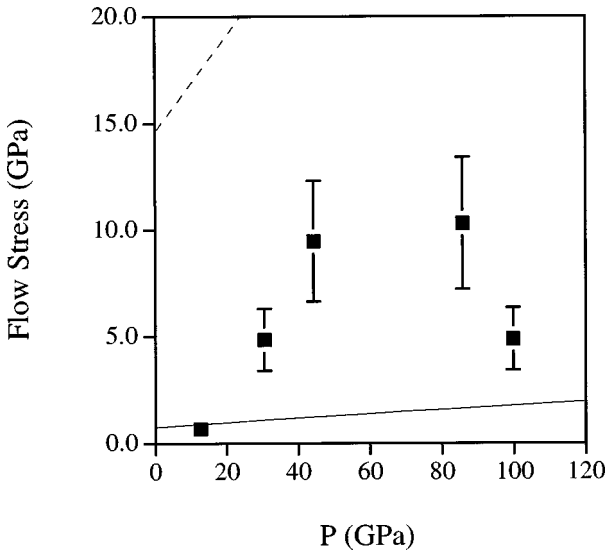

FIG. 8. Ta flow stress vs pressure (low-strain sample). Low-strain Ta flow stress data is represented by solid squares. The solid line is the Steinberg-Guinan lower limit estimate of the flow stress and the dashed line represents the calculated ideal strength of a perfect crystal (Ref. 5). The ideal strengths calculated in Ref. 5 were actually ideal *shear* strengths, so they were multiplied by a factor of 2 (Tresca yield criterion) to convert them into ideal yield strengths.

strain in the sample as it undergoes compression. The strain was examined at a radius $r=30$ μm. Figure 7 shows the results of the simulation, which is presented in the form of an equivalent plastic strain vs gasket compression h/h_0 plot where h is the gasket thickness and h_0 is the initial gasket thickness. The plastic strain in the gasket can vary somewhat as a function of axial coordinate z, and this variation is represented by the shaded region in Fig. 7, the strain being larger near the gasket-diamond interfaces than near the $z=0$ midplane. Also shown is the estimated strain expected from the equation $\varepsilon=\ln(A_0/A)$ for uniform, one-dimensional strain,[16] where A_0 is the initial cross-sectional area, and A is the final cross-sectional area of the strained specimen.

Both this NIKE2D simulation and the $\varepsilon=\ln(A_0/A)$ equation assume that the material is incompressible. Since in an actual sample some of the sample thickness reduction results from elastic compression, the strain vs gasket compression curves of Fig. 7 tend to overestimate the true amount of plastic strain. We have performed additional simulations which indicate that including the effects of compressibility may reduce the calculated plastic strains by no more than 20%. This amount is comparable to the variation of the plastic strain as a function of axial position in the sample. Therefore, for the purpose of providing estimates of the total plastic strain, we will simply state the strain values calculated assuming an incompressible sample.

IV. RESULTS

A. Tantalum strength

For Ta, we performed two experimental runs, one on a sample with an initial thickness of 25 μm, and another on a sample with an initial thickness of 50 μm. We will refer to these as the ''low-strain'' and ''high-strain'' experiments, respectively, since they are pressurized according to the different relative pressure-strain paths shown in Fig. 3. The pressure gradients were obtained by linear fits of the pressure vs radial distance data at a radial distance of approximately 20–30 μm from the high-pressure center.

TABLE I. Ta flow stress data for the low-strain experiment. The strains were estimated from NIKE2D simulations. The initial gasket thickness h_0 was 25 μm, and h was the gasket thickness under high pressure.

P (GPa)	Strain ε	h/h_0	dP/dr (GPa/μm)	Flow stress σ_0 (GPa)
12.6	0.045	0.92±0.28	0.029±0.003	0.67±0.20
30.5	0.168	0.82±0.25	0.24±0.02	4.8±1.4
44.3	0.308	0.73±0.22	0.52±0.05	9.5±2.9
85.8	0.916	0.48±0.14	0.85±0.09	10.3±3.1
99.8	1.167	0.40±0.12	0.49±0.05	4.9±1.5

The results of our low-strain Ta strength experiment are shown on the flow stress vs pressure plot of Fig. 8 and in Table I. The flow stress is only 0.67 GPa at a pressure of 12.6 GPa (estimated strain ≈5%), but then rapidly increases, reaching 10.3 GPa at a pressure of 85.8 GPa (estimated strain ≈90%). Above a pressure of 85.8 GPa, the flow stress dramatically decreases. Again, since the sample is undergoing increasing strain with increasing pressure, this decrease in flow stress may be strain related rather than pressure related. We will discuss this point further later in the paper.

Also shown in Fig. 8 is a line representing $Y_L=Y_0G_V(P)/G_V(0)$, where $Y_0(=0.77$ GPa) is the zero-pressure Steinberg-Guinan[17] value for the yield strength of

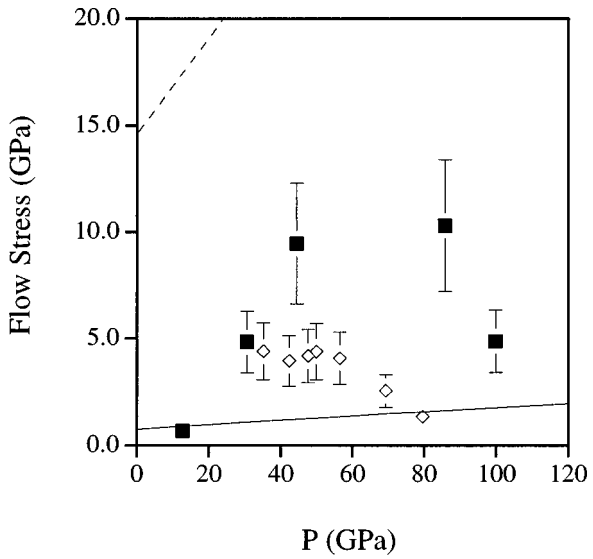

FIG. 9. Ta flow stress vs pressure (both high strain and low strain). High-strain data points are represented by diamonds, low-strain data by squares. The solid line is the Steinberg-Guinan lower limit estimate of the flow stress, and the dashed line represents the calculated ideal strength of a perfect crystal (Ref. 5). The ideal strengths calculated in Ref. 5 were actually ideal *shear* strengths, so they were multiplied by a factor of 2 (Tresca yield criterion) to convert them into ideal yield strengths.

TABLE II. Ta flow stress data for the high-strain experiment. The strains were estimated from NIKE2D simulations. The initial gasket thickness h_0 was 50 μm and h was the gasket thickness under high pressure.

P (GPa)	Strain ε	h/h_0	dP/dr (GPa/μm)	Flow stress σ_0 (GPa)
35.0	0.53	0.63±0.19	0.14±0.01	4.4±1.3
42.2	0.72	0.55±0.17	0.14±0.01	4.0±1.2
47.5	0.88	0.50±0.15	0.17±0.02	4.2±1.3
49.8	0.95	0.47±0.14	0.19±0.02	4.4±1.3
56.3	1.15	0.41±0.12	0.20±0.02	4.1±1.2
69.2	1.58	0.27±0.08	0.19±0.02	2.6±0.8
79.5	1.94	0.16±0.05	0.17±0.02	1.4±0.4

Ta, and $G_V(P)$ is the Voight-averaged shear modulus of Ta at a pressure of P. The value of Y_L, which includes pressure hardening but not strain hardening, is a reasonable lower bound on the strength of Ta.[5] An upper bound on the flow stress of Ta can also be established, and this is represented by the dashed line in Fig. 8. This line represents the calculated, first principles, ideal strength of a perfect crystal of bcc Ta, which is determined by calculating the shear stress needed to deform a crystal via the observed twinning mode of a $\langle 111 \rangle$ shear across the $\{112\}$ plane.[5]

Figure 9 shows the addition of the ''high-strain'' Ta data to the plot of Fig. 8, and Table II gives the high-strain data points. The strength along this pressure-strain path is quite different from that of the ''low-strain'' sample. We were unable to collect useful data at pressures below 35 GPa from this run because a radial pressure gradient due to sample flow was not clearly established at lower pressures. However, since the flow stress at a pressure of 35 GPa is 4.4 GPa (estimated strain $\approx$50%), much pressure hardening and strain hardening must have occurred by this pressure. As the sample is further pressurized and strained, the flow stress eventually decreases.

To examine the dislocation structure of Ta strained at high pressure, we recovered a Ta sample from a pressure of 5.0 GPa and examined the sample with TEM. Figures 10 and 11 show the TEM micrographs of this sample. In Fig. 10, a very high density of dislocations is observed with a density of the order of 5×10^{13} m/m^3. Figure 11 shows a region of the sample where the edge dislocations (Burgers vector: $\frac{1}{2}\langle 111 \rangle$) have entangled and rearranged themselves to form subgrain boundaries. These results confirm that the sample has undergone a great deal of plastic strain in the diamond-anvil cell, and that a large amount of strain hardening likely occurred. Unfortunately, due to the small size of the recovered sample ($\approx$100 μm diameter and 10 μm thick) we were unable to perform any mechanical properties testing on this sample, although efforts are underway to perform microhardness tests on future samples.

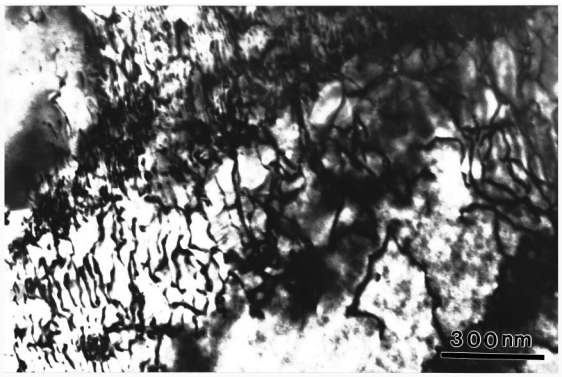

FIG. 10. TEM micrograph of Ta recovered from 5.0 GPa. A very high density of dislocation lines is evident. The estimated dislocation density is of the order of 5×10^{13} m/m^3.

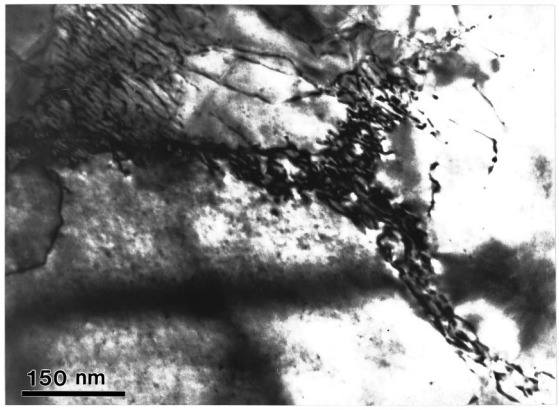

FIG. 11. TEM micrograph of Ta recovered from 5.0 GPa. A region of the recovered sample where the edge dislocations have merged to form subgrain boundaries.

B. Uranium strength

For U, we performed one experimental run on a sample with an initial thickness of 19 μm. As was done for Ta, the pressure gradients were obtained by linear fits to the pressure vs radial distance data at a radial distance of approximately 20–30 μm from the high-pressure center. The results are shown in Fig. 12 and Table III. Again, the flow stress reaches very high values (19.8 GPa at $P=109$ GPa and an estimated strain of $\approx$70%). In addition, the flow stress first increases and then decreases as the pressure and strain increase in a manner similar to that observed for Ta. No first-principles ideal strength calculations have yet been performed on U. However, ideal strengths are typically in the neighborhood of $G/10$, where G is the shear modulus. The shear modulus of U has been ultrasonically measured to 1.8 GPa and it was found that $dG/dP=2.99\pm0.11$.[18] We apply a linear extrapolation of this data to higher pressures to obtain the $G/10$ estimated ideal strength line shown in Fig. 12. Also shown is a $Y_L=Y_0G(P)/G(0)$ estimated lower strength limit line based on a Y_0 of 0.4 GPa (Ref. 17) and a linear extrapolation of the ultrasonic shear modulus data.

V. DISCUSSION

The results presented here for Ta and U reveal that the strengths of both metals reach exceptionally high values when plastically strained under ultrahigh pressures. For Ta, the flow stress reaches 10.3 GPa and for U it reaches 19.8

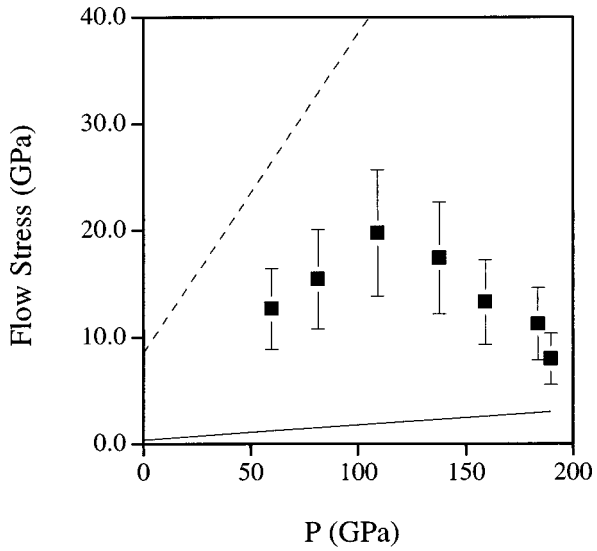

FIG. 12. U flow stress vs pressure. The solid line is the Steinberg-Guinan lower limit estimate of the flow stress, and the dashed line represents $G/10$, which is a rough estimate of the ideal strength of U.

GPa. For comparison, high strength steels at ambient pressure have tensile yield strengths up to about 2.5 GPa. Other DAC studies have obtained results similar to ours in that extremely high strengths were observed. For example, the flow stresses of W and Fe were found to be in the range of approximately 10–20 GPa at a pressure of 200 GPa.[19] For Re, the shear stress in the sample at around 100 GPa was found to be approximately 10 GPa,[20] which translates into a flow stress of about 20 GPa.

It is interesting to compare the measured flow stresses with the expected upper and lower bounds on strength (Figs. 8, 9, and 12). Although the measured strengths are extremely high, they are still below the ideal strength limits predicted by theoretical calculations or by $G/10$ scaling arguments. For both Ta and U, the flow stresses remain below about $G/20$. If we now compare the measured flow stresses with the Y_L lower limit bounds on the strength, we see that the measured flow stresses are up to ten times higher than the Y_L lines, which assume no strain hardening. Tantalum, being a bcc metal, does not normally exhibit much strain hardening in comparison to fcc metals. However, Bridgeman[1] found that the flow stress of Ta under high pressure (pressures up to 3 GPa) increased by about a factor of 3 due to strain hardening. The final strain was approximately 200%, and was limited by geometrical irregularities which started to appear in the neck of the Ta rod. In our experiments, we find that the flow stress of Ta at 86 GPa is about six times higher than that expected on the basis of pressure hardening alone. The estimated strain at this pressure was ≈90%. These results suggest that the strain hardening of Ta is very pressure dependent.

TABLE III. U flow stress data. The strains were estimated from NIKE2D simulations. The initial gasket thickness h_0 was 19 μm, and h was the gasket thickness under high pressure.

P (GPa)	Strain ε	h/h_0	dP/dr (GPa/μm)	Flow stress σ_0 (GPa)
59.6	0.25	0.77±0.23	0.87±0.09	12.7±3.8
81.4	0.41	0.68±0.20	1.19±0.12	15.5±4.7
109.0	0.67	0.57±0.17	1.82±0.18	19.8±5.9
137.5	0.98	0.46±0.14	1.99±0.20	17.5±5.3
158.9	1.23	0.38±0.11	1.85±0.19	13.3±4.0
183.4	1.54	0.28±0.08	2.10±0.21	11.3±3.4
189.6	1.62	0.26±0.08	1.62±0.16	8.0±2.4

Strain softening. We observed that at the highest pressures and strains both Ta and U exhibit decreases in the flow stress. We interpret this decrease as a strain-related effect. For all three experimental runs, the drop in the flow stress occurs when the estimated strain is in the neighborhood of 100%. Bridgeman[1] also observed decreases in the flow stress at strains ranging from 100 to 200 % in nickel, molybdenum, and tungsten, and he termed the effect ''strain softening.'' A large strain-softening effect was also observed in strength experiments on MgO using a DAC.[11] The cause of this strain-softening effect is not yet clear. On the basis of visual observations of the recovered samples, Bridgeman[1] concluded that the cause was material damage induced in highly strained specimens due to ''a lack of homogeneity in the original material,'' presumably at the grain size level. In the case of the DAC experiment on MgO, the observed strain softening was explained in terms of preferred grain orientation of the easy slip planes.[11] It is unclear which explanation holds for our Ta and U data, and further experiments will be needed to resolve this point.

VI. CONCLUSION

In summary, we have performed high-pressure flow stress experiments on Ta and U to 99.8 and 189.6 GPa, respectively. The flow stress of Ta reaches 10.3 GPa at a pressure of 85.8 GPa and an estimated strain of ≈90%. The flow stress of U reaches 19.8 GPa at a pressure of 109.0 GPa and an estimated strain of ≈70%. These flow stresses are up to ten times higher than expected on the basis of pressure hardening alone, which suggests that strain hardening under high pressure is a very important factor. Additionally, we find that the flow stress starts to decrease at higher strains and pressures when the strain reaches the neighborhood of 100%. This strain-softening effect has also been observed in other high-pressure experiments on other materials, and it has been suggested that the effect is due to either material damage at high strains or to preferential grain orientation. Further studies will be needed to determine the mechanism responsible for strain softening in the case of Ta and U.

ACKNOWLEDGMENTS

We thank W. King, B. Bonner, D. Farber, and J. Zaug for valuable discussions. Also, we thank Dr. Jing Zhu Hu for valuable discussions and technical assistance. Finally, we thank B. T. Goodwin and L. Wiley for their support. This research was supported by B-Division at Lawrence Livermore National Laboratory under the auspices of the U.S. Department of Energy under Contract No. W-7405-ENG-48.

[1] P. W. Bridgeman, J. Appl. Phys. **24**, 560 (1953).
[2] P. W. Bridgeman, *Studies in Large Plastic Flow and Fracture* (McGraw-Hill, New York, 1952).
[3] J. O. Chua and A. L. Ruoff, J. Appl. Phys. **46**, 4659 (1975).
[4] *Mechanical Behavior of Materials under Pressure*, edited by H. Pugh (Elsevier, New York, 1970), pp. 256–262.
[5] P. Soderlind and J. Moriarty, Phys. Rev. B **57**, 10 340 (1998).
[6] G. H. Campbell, S. M. Foiles, H. Huang, D. A. Hughes, W. E. King, D. H. Lassila, D. J. Nikkel, T. Diaz de la Rubia, J. Y. Shu, and V. P. Smyshlyaev (unpublished).
[7] W. E. King, G. Campbell, T. Gonis, G. Henshall, D. Lesuer, E. Zywicz, and S. Foiles, Mater. Sci. Eng., A **191**, 1 (1995).
[8] J. Xu, H. Mao, and P. Bell, High Temp.-High Press. **16**, 495 (1984).
[9] J. Akella, G. S. Smith, R. Grover, Y. Wu, and S. Martin, High Press. Res. **2**, 295 (1990).
[10] C. Sung, C. Goetze, and H. Mao, Rev. Sci. Instrum. **48**, 1386 (1977).
[11] C. Meade and R. Jeanloz, J. Geophys. Res. **93**, 3261 (1988).
[12] If the gasket thickness is reduced by a factor of 2, a roughly 100% strain is expected from the application of $\varepsilon = \ln(A_0/A)$ where A_0 is the original cross-sectional area and A is the final cross-sectional area of a strained sample. This was confirmed by a NIKE2D finite element calculation, which gave 90–120 % equivalent plastic strain.
[13] J. B. Engelman, NIKE2D: *A Non-Linear, Implicit, Two-Dimensional, Finite Element Code for Solid Mechanics* (unpublished).
[14] W. C. Moss, J. O. Hallquist, R. Reichlin, K. A. Goettel, and S. Martin, Appl. Phys. Lett. **48**, 1258 (1986).
[15] W. C. Moss and K. A. Goettel, Appl. Phys. Lett. **50**, 25 (1987).
[16] J. Vernon, *Introduction to Engineering Materials*, 3rd ed. (MacMillan, London, 1994), pp. 452–453.
[17] D. J. Steinberg, S. G. Cochran, and M. W. Guinan, J. Appl. Phys. **51**, 1498 (1980).
[18] A. E. Abey and B. P. Bonner, J. Appl. Phys. **46**, 1427 (1975).
[19] R. J. Hemley, H. Mao, G. Shen, J. Badro, P. Gillet, M. Hanfland, and D. Hausermann, Science **276**, 1242 (1997).
[20] R. Jeanloz, B. K. Godwal, and C. Meade, Nature (London) **349**, 687 (1991).